Charge-dependent flow and the search for the chiral magnetic wave in Pb-Pb collisions at root s(NN)=2.76 TeV

Adam, J.; Adamova, D.; Aggarwal, M.M.; Rinella, G.A.; Agnello, A.; Agrawal, N.; Ahammed, Z.; U. Ahn, S.; Aiola, S.; Akindinov, A.; Alessandro, B.; Alexandre, H.; Alfaro Molina, R.; Bearden, Ian; Bøggild, Hans; Christensen, Christian Holm; Gulbrandsen, Kristjan Herlache; Gaardhøje, Jens Jørgen; Dalsgaard, Hans Hjersing; Nielsen, Børge Svane; Hansen, Alexander Colliander; Bilandzic, Ante; Chojnacki, Marek; Zaccolo, Valentina; Zhou, You; Bourjau, Christian Alexander

Published in:
Physical Review C - Nuclear Physics

DOI:
10.1103/PhysRevC.93.044903

Publication date:
2016

Document version
Publisher's PDF, also known as Version of record

Charge-dependent flow and the search for the chiral magnetic wave in Pb-Pb collisions at $\sqrt{s_{NN}} = 2.76$ TeV

J. Adam *et al.*[*]
(ALICE Collaboration)

(Received 18 December 2015; published 8 April 2016)

We report on measurements of a charge-dependent flow using a novel three-particle correlator with ALICE in Pb-Pb collisions at the CERN Large Hadron Collider (LHC), and discuss the implications for observation of local parity violation and the chiral magnetic wave (CMW) in heavy-ion collisions. Charge-dependent flow is reported for different collision centralities as a function of the event charge asymmetry. While our results are in qualitative agreement with expectations based on the CMW, the nonzero signal observed in higher harmonics correlations indicates a possible significant background contribution. We also present results on a differential correlator, where the flow of positive and negative charges is reported as a function of the mean charge of the particles and their pseudorapidity separation. We argue that this differential correlator is better suited to distinguish the differences in positive and negative charges expected due to the CMW and the background effects, such as local charge conservation coupled with strong radial and anisotropic flow.

DOI: 10.1103/PhysRevC.93.044903

I. INTRODUCTION

Parity (P) is a major symmetry of classical physics, being present in rigid-body dynamics, classical electrodynamics, and gravity. In the development of quantum mechanics, parity conservation was assumed. It was not until the 1950s [1] that the possibility of parity violation was considered, and soon after it was definitively demonstrated experimentally in nuclear decays [2,3]. In the modern picture, P and CP violation in weak interactions are widely established experimentally and well understood theoretically. In strong interactions there is very little or no global P violation, as determined by measurements of the neutron electric dipole moment [4,5]. However, there is no first-principles reason why P and CP violation should not exist in strong interactions. P and CP violation as a general feature of quantum field theories was first explored in the 1970s [6,7], and a proposal to use heavy-ion collisions as a tool for studying P and CP violation first appeared as early as the 1980s [8]. Specific proposals for a search for local P-violating effects in heavy-ion collisions appeared in the last decade [9–14].

Collisions of heavy nuclei at ultrarelativistic energies create a hot, dense medium that appears to have partonic degrees of freedom and evolve hydrodynamically. In noncentral collisions the initial overlap region is nonisotropic, which, due to particle interactions, leads to a momentum-space anisotropy of the produced particles. This anisotropy can be described using a Fourier expansion of the azimuthal distribution of particles [15]. Noncentral collisions are also characterized by large orbital momentum and, of importance to this study, very large magnetic fields. Numerical estimates [16,17] indicate that at CERN Large Hadron Collider (LHC) energies the field strength can be as large as $B \approx m_\pi^2/e \approx 10^{14}$ T. In a vacuum, the magnetic field induced by the spectators decays in time quadratically ($B \propto t^{-2}$) and the lifetime of the magnetic field at LHC energies is extremely short, decreasing six orders of magnitude over the course of 0.5 fm/c. However the presence of electrical charges (such as the quarks in the QGP) means there is finite electrical conductivity. By Lenz's law the change in magnetic field is opposed by the charge carriers in the conductor, so the temporal decay of the magnetic field is significantly slowed [18,19].

The chiral magnetic effect (CME) [20] is a process of charge separation with respect to the reaction plane. In the QCD vacuum there can exist gluonic configurations with nonzero topological charge, which can be an instanton or a sphaleron. At high temperatures, the sphaleron rate is expected to be dominant. The presence of such gluonic configurations with topological charge is what drives the P-violation process. For example, in a region with negative topological charge, left-handed quarks will become right-handed, and right-handed quarks will remain right-handed. The strong magnetic field created in heavy-ion collisions interacts with the magnetic moment of the quarks and orients the spins of quarks with positive (negative) electric charge to be parallel (antiparallel) to the field direction. Under the assumption of massless quarks, right-handed quarks have their spins and momenta aligned. This will cause positive (negative) quarks to move parallel (antiparallel) to the magnetic field, leading to a positive electric current and thus a positive electric charge dipole. Due to the chiral symmetry restoration, u and d quarks have only their bare Higgs mass, which is of the order of a few MeV/c^2. This is sufficiently small to regard the quarks as effectively massless. Based on simple geometrical arguments, the magnetic field direction is always normal to the reaction plane, and therefore straightforwardly accessible to experiment. The chiral separation effect (CSE) [21] is a similar effect in which the presence of a vector charge, e.g.,

[*]Full author list given at the end of the article.

electric charge, causes a separation of chiralities. For example, the presence of a net positive electric charge will induce a positive axial current along the direction of the magnetic field, i.e., right (left) handed quarks moving parallel (antiparallel) to the magnetic field.

The CME can be summarized in a relatively simple equation:

$$\vec{J}_V = \frac{N_c e}{2\pi^2}\mu_A \vec{B}, \tag{1}$$

where $\vec{J}_V$ is the vector current (electric charge current in this case), N_c is the number of colors [3 in QCD but other numbers of colors, i.e., SU(N_c) gauge fields, are of interest in theory], μ_A is the axial chemical potential (which encodes the anomaly-induced chiral imbalance), and $\vec{B}$ is the magnetic field. The CSE can similarly be summarized as

$$\vec{J}_A = \frac{N_c e}{2\pi^2}\mu_V \vec{B}, \tag{2}$$

where $\vec{J}_A$ is the axial current (flow of axial charges, i.e., chiralities) and μ_V is the vector (electric) chemical potential. The coupling between these two phenomena leads to a wave propagation of the electric charge, resulting in an electric charge quadrupole moment of the system. This is called the chiral magnetic wave (CMW) [22–24]. Importantly, for a given (net) charge state of the system, the quadrupole moment always has the same sign and is therefore present in an average over events with the same vector charge state, meaning it may lead to a signal strong enough to be observed directly in experiment.

As mentioned above, the azimuthal distribution of particles can be written as a Fourier expansion:

$$\frac{dN}{d\varphi} \propto 1 + \sum_n 2v_n \cos[n(\varphi - \psi_n)], \tag{3}$$

where φ is the azimuthal angle of the particle, v_n is the Fourier coefficient, and ψ_n is the symmetry plane, which in principle can be different for each harmonic number n.

Taking into account the well-known modulation of particle emission due to elliptic flow parameterized with the Fourier coefficient v_2 (see, e.g., [25]), one can write the azimuthal distribution of charged particles due to the CMW [24] as

$$\frac{dN^\pm}{d\varphi} = N^\pm[1 + (2v_2 \mp rA)\cos(2(\varphi - \psi_2))], \tag{4}$$

where the charge asymmetry $A = (N^+ - N^-)/(N^+ + N^-)$ is determined in some kinematic region (for example in the experimental acceptance), and the parameter r encodes the strength of the electric quadrupole due to the CMW. Bjorken flow [26] relates the pseudorapidity of a particle to its longitudinal production point. Due to space-momentum correlations, the charge asymmetry A, determined in the experimental acceptance, corresponds to the local charge asymmetry in a certain region of the fireball.

ALICE measurements of the charge dependent correlations in search for the CME have been published in [27]. This paper presents the ALICE results on the charge dependent elliptic flow as a function of the event charge asymmetry. As the event charge asymmetry A strongly depends on the experimental acceptance and tracking efficiency, we also present related results on a differential three-particle correlator that allows much more detailed study of the underlying physics mechanisms. We also present the corresponding measurements for higher harmonics flow that should be largely insensitive to the CMW but sensitive to the possible background effects.

II. ANALYSIS METHODOLOGY

A. v_n as a function of A and integral three-point correlators

In the theoretical work on the CMW [22–24,28,29] as well as the analysis published by STAR [30] of Au-Au collisions at $\sqrt{s_{NN}} = 200$ GeV, the observable has been the charge-dependent flow coefficient $v_n^\pm$ as a function of the charge asymmetry A. Experimentally, the charge asymmetry defined in a specified kinematic region must be corrected for detector efficiency, as discussed in [30–32]. The effect of the correction is to increase the slope of positive or negative particle $v_n^\pm$ vs A. This correction to the slope, though absolutely necessary, has the undesired feature of introducing additional sources of systematic uncertainty.

In addition to measuring $v_n^\pm$ as a function of A for a specified event-selection criterion (e.g., a centrality interval), one can measure the covariance of $v_n^\pm$ and A, i.e., $\langle v_n^\pm A\rangle - \langle A\rangle\langle v_n^\pm\rangle$, as a function of some event-level variable (e.g., centrality) [33]. The harmonic coefficient is, by definition, $v_n = \langle\cos[n(\varphi_1 - \psi_n)]\rangle$, where φ_1 is the azimuthal angle of a particle in the event and ψ_n is the th harmonic symmetry plane. This makes $\langle v_n^\pm A\rangle - \langle A\rangle\langle v_n^\pm\rangle$ a three-point correlator. The first point is the flow particle, the second point is the event plane (which is an estimator for the true symmetry plane), and the third point is the event charge asymmetry. In cases where the event plane is determined with a second particle, as is the case with the two-particle cumulant method, this correlator can also be called a three-particle correlator.

The strength of the covariance of any two variables is independent of the sample size as long as the correlation is statistically significant, so no correction for efficiency is needed for the three-point correlator. For that reason, the correlation strength is identical for the full set of particles in some collection of events and for some randomly selected subset of particles in the same collection of events [34].

From Eq. (4), it follows that $v_2^\pm \approx \overline{v}_2 \mp rA/2$, which in turn allows one to write $\Delta v_2 = v_2^- - v_2^+ \approx rA$. By measuring Δv_2 as a function of A, it is possible to extract r directly in experiment. One can also substitute these terms into the three-particle correlator, giving

$$\langle v_2^\pm A\rangle - \langle A\rangle\langle v_2^\pm\rangle \approx \mp r(\langle A^2\rangle - \langle A\rangle^2)/2 = \mp r\sigma_A^2/2. \tag{5}$$

Clearly, either of these approaches can be generalized to arbitrary harmonic v_n, yielding in principle a different r for each harmonic. Because of the symmetry of the CMW effect, the expectation is that r, and therefore the three-particle correlator, is significant only for the second harmonic and strongly suppressed for higher harmonics. Since A is efficiency dependent, it is necessary to scale down the observed width to account for the natural broadening due to the binomial sampling. To calculate the scale factor, we compared the

widths of A in a Monte Carlo simulation before and after reconstruction effects, where the full detector response was implemented within the GEANT3 [35] framework. Since the ALICE tracking efficiency is independent of centrality, this scale factor is also independent of centrality. This correction to σ_A^2 introduces an additional source of systematic uncertainty, in essentially the same way as the correction to the slope for $v_n^{\pm}$ vs A. In the present analysis, this uncertainty represents a roughly 6% normalization uncertainty on the points. Both the correction and the associated uncertainty vary depending on detector acceptance and efficiency, analysis cuts, etc. A key advantage of measuring the three-particle correlator, rather than r (directly or indirectly), is that it is efficiency independent and does not require any correction. This reduces the overall systematic uncertainty on the measurement, which better facilitates comparisons across experiments as well as with theory calculations.

In this analysis, two-particle cumulants are always used to calculate v_n [which ignores correlations not related to anisotropic flow (nonflow), as well as flow fluctuations]. Then, the integral correlator is

$$\begin{aligned}\langle v_n^{\pm} A\rangle - \langle A\rangle\langle v_n\rangle &= \langle \cos[n(\varphi_1 - \psi_n)]\, A\rangle \\ &\quad - \langle \cos[n(\varphi_1 - \psi_n)]\rangle\langle A\rangle \\ &\approx \frac{\langle\langle \cos[n(\varphi_1 - \varphi_2)] A\rangle\rangle}{\sqrt{\langle\langle \cos[n(\varphi_1 - \varphi_2)]\rangle\rangle}} \\ &\quad - \sqrt{\langle\langle \cos[n(\varphi_1 - \varphi_2)]\rangle\rangle}\langle A\rangle. \end{aligned} \quad (6)$$

For this equation the inner average represents an average over all particles in a single event, and the outer average represents an average over all events. The first particle has the selected charge and the second particle is of both charges. For the integral correlator reported below, the same particles are used to calculate v_n and A. The slopes extracted from the three-particle correlator were checked against the slopes extracted directly from Δv_2 vs A and found to be perfectly consistent with each other.

B. Differential three-point correlators

A key advantage of the novel three-point correlator is that it permits more differential studies and as such has more discriminating power. The charge asymmetry in the event can be generalized to the charge of a particle in the event, which we will call q_3. The average of all charges in the event is equal to the charge asymmetry, i.e., $\langle q_3\rangle_{\text{event}} \equiv A$. Under this generalization the correlator [Eq. (6)] becomes $\langle v_n q_3\rangle - \langle q_3\rangle\langle v_n\rangle$.

We also use the additional notation of $\langle q_3\rangle_1$ to denote the mean of q_3 evaluated when selecting on the charge of the first particle q_1. This is important because, by construction, the correlator $\langle v_n q_3\rangle - \langle q_3\rangle\langle v_n\rangle$ contains reducible correlations, i.e., correlations that can be expressed in terms of lower order correlations [33,34]. These reducible correlations are removed by the construction $\langle v_n q_3\rangle - \langle q_3\rangle_1\langle v_n\rangle$, which is therefore a three-point cumulant.

Using these relations, we estimate the differential correlator in the following way:

$$\begin{aligned}&\langle v_n^{\pm} q_3\rangle - \langle q_3\rangle_1\langle v_n\rangle \\ &\quad = \langle \cos[n(\varphi_1 - \psi_n)]\, q_3\rangle - \langle \cos[n(\varphi_1 - \psi_n)]\rangle\langle q_3\rangle_1 \\ &\quad \approx \frac{\langle\langle \cos[n(\varphi_1 - \varphi_2)] q_3\rangle\rangle}{\sqrt{\langle\langle \cos[n(\varphi_1 - \varphi_2)]\rangle\rangle}} - \sqrt{\langle\langle \cos[n(\varphi_1 - \varphi_2)]\rangle\rangle}\langle q_3\rangle_1. \end{aligned} \quad (7)$$

The evaluation of a differential correlator is a very important feature of this study. Rather than measuring only event quantities, one can also measure the relationship between the flow at a particular kinematic coordinate and the charge of the third particle at another particular coordinate. This means the effect can be measured as a function of the separation in pseudorapidity of particles 1 and 3, for example. This differential nature allows for a much more detailed study of the origin of the correlation and provides stronger experimental constraints on the theoretical modeling of such effects.

Throughout this paper we use the subscript notation used above for the first, second, and third particles. The charge, azimuthal angle, and pseudorapidity of the first particle are q_1, φ_1, and η_1, respectively. Similarly, the azimuthal angle of the second particle is φ_2, and the charge and pseudorapidity of the third particle are q_3 and η_3, respectively.

III. EXPERIMENTAL APPARATUS AND DATA ANALYSIS

ALICE [36,37] is a dedicated heavy-ion experiment located at the Large Hadron Collider at CERN. It is composed of a wide array of detector subsystems. Those used in the present analysis are the V0 detectors, the Inner Tracking System (ITS), and the Time Projection Chamber (TPC). The V0 detectors consist of scintillator arrays and are used for triggering and centrality determination. There are two V0 detectors, V0A and V0C. The V0A is located 340 cm from the nominal interaction point and the V0C is installed at 90 cm distance in the opposite direction. The V0A covers $2.8 < \eta < 5.1$ in pseudorapidity

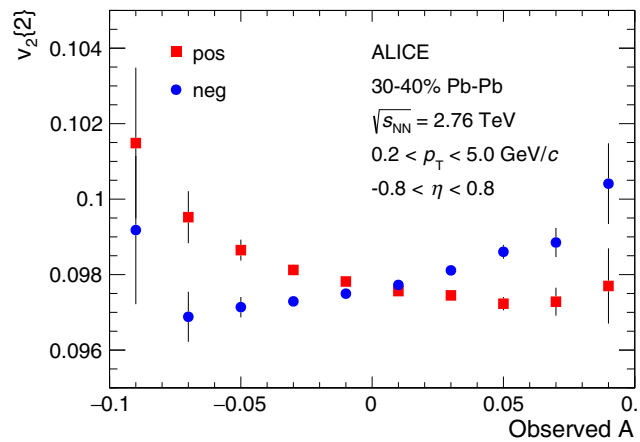

FIG. 1. Harmonic coefficients v_2^+ (red squares) and v_2^- (blue circles) as a function of the observed event charge asymmetry A in the 30–40% centrality class. Statistical uncertainties only.

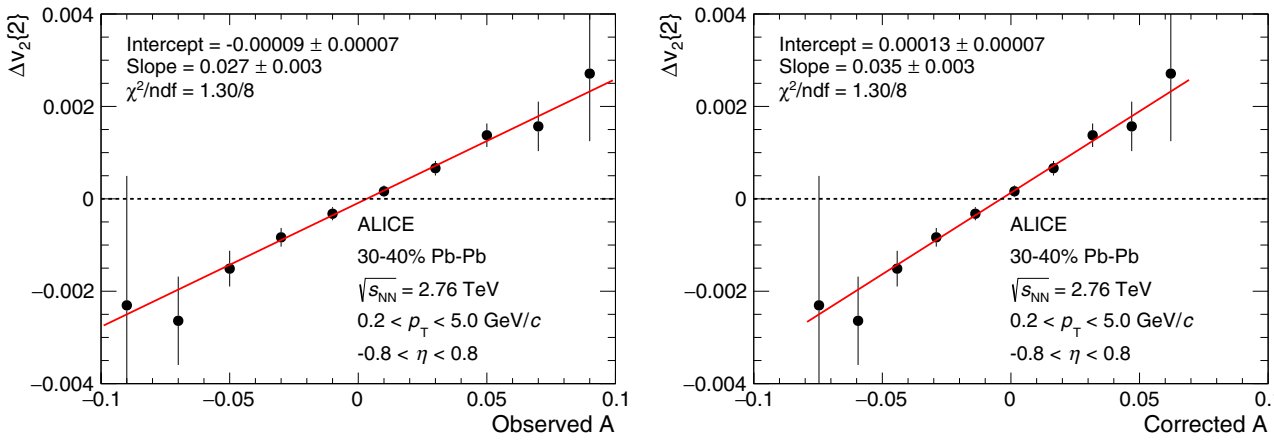

FIG. 2. $\Delta v_2 = v_2^- - v_2^+$ as a function of the observed (left) and corrected (right) event charge asymmetry A in the 30–40% centrality class. Statistical uncertainties only.

and the C side spans $-3.7 < \eta < -1.7$. The ITS is used for both tracking and vertex determination. The ITS is composed of three subsystems, each having two cylindrical layers of silicon detectors. Each of the layers covers at least $|\eta| < 0.9$ in pseudorapidity to match the TPC acceptance. The TPC is the primary tracking detector at midrapidity. The TPC is a large gas volume detector separated into two regions by a central electrode, positioned in a solenoidal magnetic field of 0.5 T. The gas volume is contained in a cylindrical electric field cage with an inner radius of 85 cm and an outer radius of 2.5 m, spanning the full azimuth $0 < \varphi < 2\pi$. It extends 5.0 m in the z direction, providing coverage of the full radial track length for pseudorapidity $|\eta| < 0.9$.

The present manuscript reports an analysis of Pb-Pb collisions at $\sqrt{s_{NN}} = 2.76$ TeV, collected by ALICE during the 2010 and 2011 years of LHC operations. In the early part of the 2010 operation, the Pb-Pb minimum bias (MB) trigger was a 2-out-of-3 coincidence of (a) signals in two pixel chips in the outer layer of the SPD, (b) a signal in the V0A, (c) a signal in the V0C. In the later part of the 2010 operation and for all of the 2011 operation, the Pb-Pb MB trigger required a coincidence of both V0 detectors. The data sample used in this analysis comprises approximately 1.7×10^7 MB triggered events in the 2010 data set. In the 2011 set, we use a mix of the central, semicentral, and MB triggers. The central trigger is an online trigger with a threshold on the multiplicity in the V0 detectors such that it corresponds to the 10% most central events. The semicentral trigger is defined similarly such that it corresponds to the 50% most central events. The centrality is estimated using the mean multiplicity in the V0 detectors, and the centrality is required to be within 5% (absolute) of the centrality estimate using the TPC multiplicity to avoid multiplicity fluctuations in the central region. The longitudinal position of the primary vertex is required to be within 10 cm of the nominal center of the ALICE coordinate system in order to ensure uniform detector acceptance.

Tracks are selected in the kinematic region $|\eta| < 0.8$ and $0.2 < p_T < 5.0$ GeV/c. They are required to have at least 70 TPC clusters, and the percentage of hits to crossed pad rows is required to be at least 80%. The track fit is required to have χ^2 per cluster (2 degrees of freedom) less than 4.0. Additional tracking information from the ITS is used when it is available, i.e., when the track trajectory in the TPC points to an active area of the ITS. The distance of closest approach to the reconstructed vertex is required to be within 3.2 cm in the z direction and within 2.4 cm in the xy-plane. Due to the excellent azimuthal uniformity of the TPC response, no correction for azimuthal acceptance is needed, nor is one applied. The results are corrected for the p_T dependence of the tracking efficiency, which is about 80% at low p_T and about 90% at high p_T. The correction procedure is to randomly exclude tracks in such a way that the effective efficiency is made to be uniform in p_T. The result is a 2–3% reduction in v_n.

To assess systematic uncertainties, the analysis is repeated for different operational conditions (i.e., the two orientations of the experimental magnetic field), different event selection criteria, different track selection cuts, and different track reconstruction methods. The uncertainties associated with each specific selection or condition are observed to be uncorrelated and thus added in quadrature to determine the overall

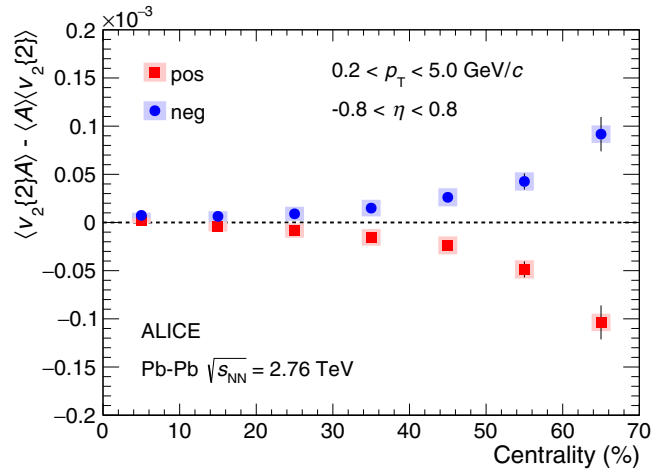

FIG. 3. Three-particle correlator for positive (red squares) and negative (blue circles) particles for the second harmonic as a function of centrality. Statistical (systematic) uncertainties are indicated by vertical bars (shaded boxes).

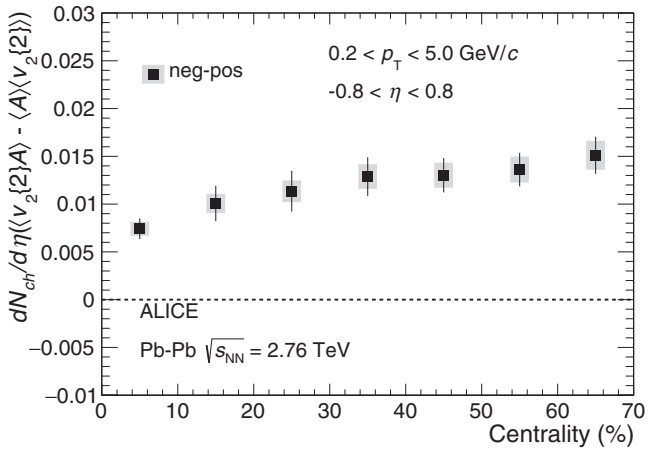

FIG. 4. Charge difference of the three-particle correlator for the second harmonic as a function of centrality, multiplied by $\langle dN_{\rm ch}/d\eta\rangle$ [39]. Statistical (systematic) uncertainties are indicated by vertical bars (shaded boxes).

systematic uncertainty. All aforementioned sources were found to generally contribute with similar magnitude. Many observables reported in this manuscript have values very close to zero, so that reporting systematic uncertainties as a percentage of these values obscures their true meaning. For numerical stability, systematic uncertainties are evaluated as a percentage of $\langle v_n\rangle\langle A\rangle$ or $\langle v_n\rangle\langle q_3\rangle$. This quantity alone is not necessarily physically meaningful, because it contains detector specific effects. It does, however, set a natural scale for the uncertainties. Once uncertainties are assessed, their absolute value is determined and then plotted together with the data points.

IV. RESULTS

A. v_2 vs A

Figure 1 shows v_2^+ and v_2^- as a function of the observed (uncorrected) event charge asymmetry A in the 30–40% centrality class. Clearly visible is an increase in v_2^- with increasing A, along with a corresponding decrease in v_2^+. This is qualitatively consistent with expectations from the CMW [22–24,28,29] as well as with the STAR results [30]. Visually the relationship does not appear exactly linear for either charge. For a given centrality selection, there is some range of multiplicities. Since A is a combination of numbers of particles, it is a combination of different negative binomial distributions, which are broader for lower numbers of particles. Therefore, for larger values of $|A|$, one is sampling events with lower multiplicities, which can affect the value of v_2.

Figure 2 shows $\Delta v_2 = v_2^- - v_2^+$ as a function of the observed A in the left panel and of A corrected for efficiency in the right panel. To obtain the corrected A, we analyzed HIJING [38] simulations propagated through a detector description implemented in the GEANT3 [35] framework to determine the true (generated particle level) A as a function of the observed (reconstructed track level) A. It can be seen that the effect of the correction is a modest increase in the slope. Again, these results are qualitatively consistent with CMW expectations and with the STAR data [30].

B. Integral correlator results as a function of centrality

Considering the observed increase (decrease) of v_2^- (v_2^+) with increasing A, discussed in the preceding section, we expect a positive (negative) covariance of v_2^- (v_2^+) with A, and indeed this is exactly what is seen in the integral correlator. Additionally, it enables a convenient study of the evolution of the correlation as a function of event-level observables.

Figure 3 shows the integral correlator of the second harmonic as a function of centrality. A substantial increase in the correlation strength is seen as the collisions become more peripheral. This can be caused by a combination of several factors. The magnetic field strength increases as the impact parameter increases since there are more spectators and thus the current gets stronger. This would cause the correlations due to the CMW to get stronger. Additionally, local charge conservation (LCC) effects could play a role [33]. It is important to note that neither of these necessarily comes at the expense of the other; in principle the observable

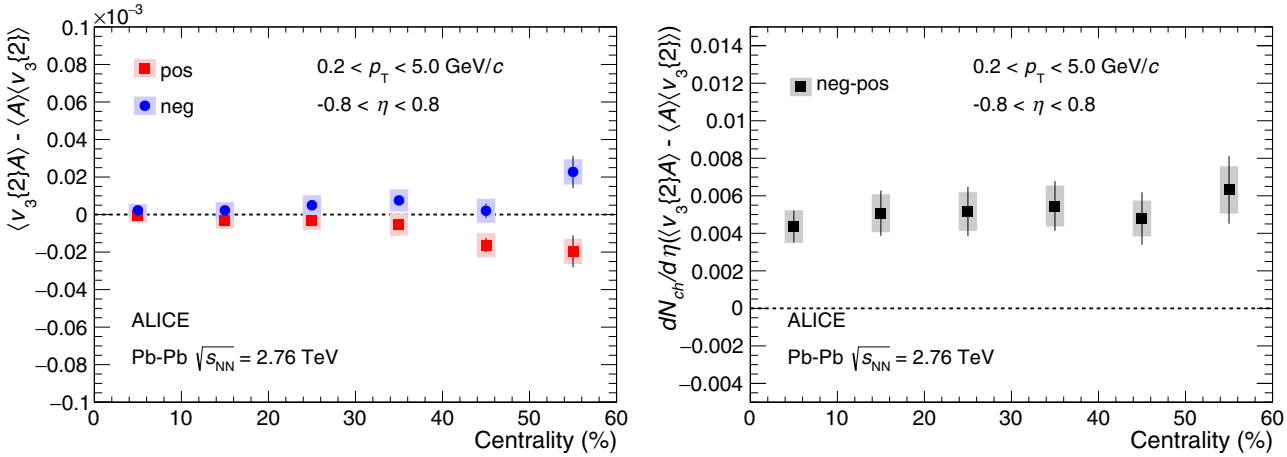

FIG. 5. Three-particle correlator for the third harmonic (left panel) for positive (red squares) and negative (blue circles) particles, and the charge difference multiplied by $\langle dN_{\rm ch}/d\eta\rangle$ (right panel). Statistical (systematic) uncertainties are indicated by vertical bars (shaded boxes).

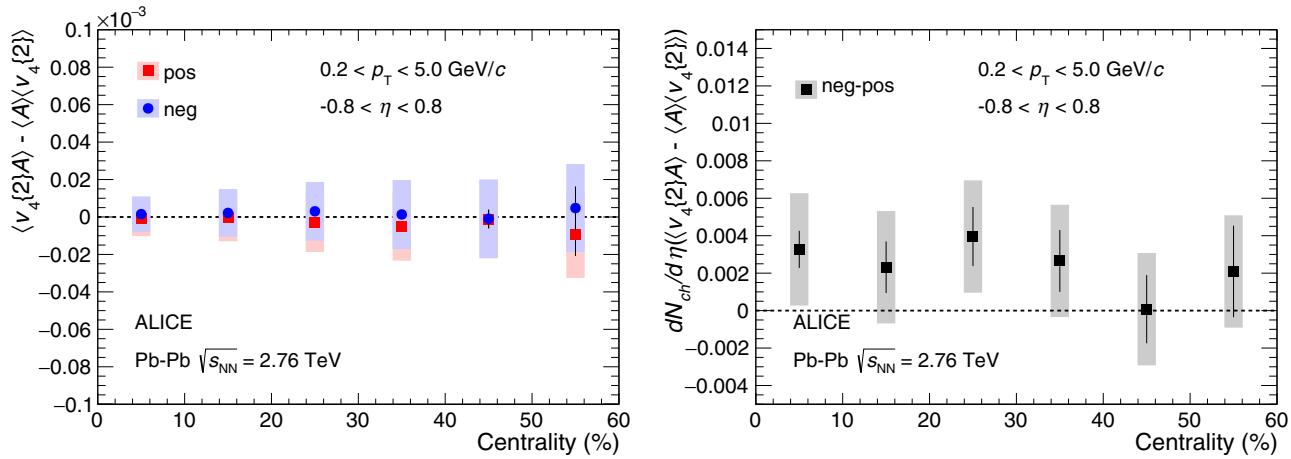

FIG. 6. Three-particle correlator for the fourth harmonic (left panel) for positive (red squares) and negative (blue circles) particles, and the charge difference multiplied by $\langle dN_{\rm ch}/d\eta\rangle$ (right panel). Statistical (systematic) uncertainties are indicated by vertical bars (shaded boxes).

could have contributions from both of these and/or additional contributions from as yet unknown sources of correlation.

Local charge conservation is the production of charged pairs at the same spacetime point. For N particles, there are $N/2$ correlated pairs, and $N(N-1)$ combinatoric pairs, meaning the correlation strength is proportional to $N/[N(N-1)]$, or approximately $1/N$. Figure 4 shows the difference between the charges for the second harmonic correlator multiplied by $\langle dN_{\rm ch}/d\eta\rangle$ [39], where $\langle dN_{\rm ch}/d\eta\rangle$ is used as a proxy for the total number of particles, to examine the role of the dilution of LCC correlations on the correlator. Considerable centrality dependence remains.

The three-particle correlator is studied using other harmonics as well. This provides important additional constraints because P-violating effects are expected to occur with respect to the reaction plane, therefore higher harmonics should have very little or no correlations. The three-particle correlator for the third harmonic is shown in Fig. 5 and the fourth harmonic is shown in Fig. 6. In both cases the left panel shows the correlator for positive and negative charges separately, and the right panel shows the charge difference of the correlator multiplied by $\langle dN_{\rm ch}/d\eta\rangle$. In both of these cases, the centrality dependence of the charge dependence is flat, in contrast to the second harmonic. This may suggest a different nature of the correlation. It could also reflect a weaker centrality dependence of v_3 compared to that of elliptic flow.

C. Slopes of Δv_2 vs A

Figure 7 shows a comparison between slope parameters r estimated in this analysis and from the STAR analysis [30] of Au-Au collisions at $\sqrt{s_{NN}} = 200$ GeV. For the STAR data, the v_2 is evaluated for charged pions with $0.15 < p_{\rm T} < 0.5$ GeV/c, in contrast with the present results which are for unidentified hadrons with $0.2 < p_{\rm T} < 5.0$ GeV/c. Overall, the slopes are surprisingly similar when considering the different collision energies and multiplicities, as well as the different kinematic acceptance (in addition to the different $p_{\rm T}$ selection, the STAR results correspond to the pseudorapidity range $|\eta| < 1.0$). The STAR data exhibit a somewhat stronger centrality dependence than the ALICE data. Moreover, the

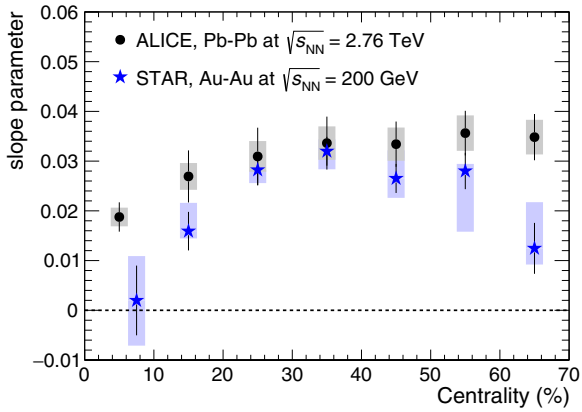

FIG. 7. Slope parameter r as a function of centrality, including points from STAR [30]. Statistical (systematic) uncertainties are indicated by vertical bars (shaded boxes). Not shown is the 6% systematic normalization uncertainty due the MC correction for σ_A^2.

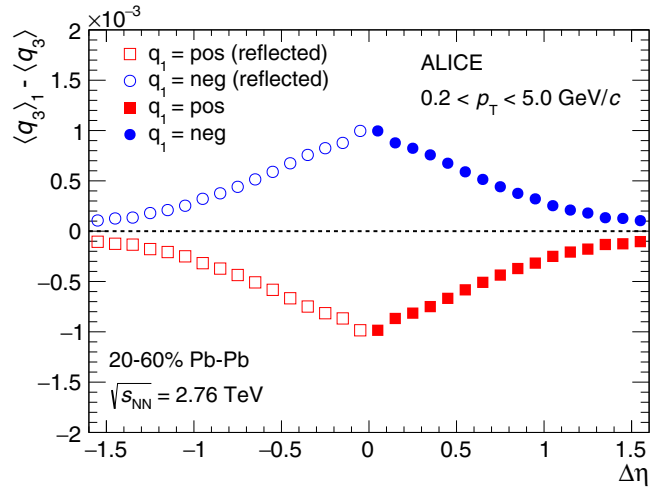

FIG. 8. Correlation between the charge of the first particle q_1 and the charge of the third particle q_3. Statistical uncertainties only.

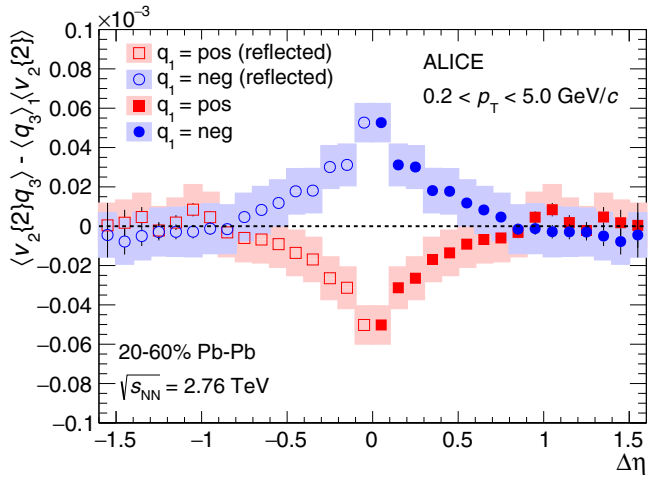

FIG. 9. Three-particle correlator for the second harmonic, for positive (red squares) and negative (blue circles) particles. Statistical (systematic) uncertainties are indicated by vertical bars (shaded boxes).

STAR data exhibit a stronger centrality dependence than predicted by the theoretical models invoking the CMW for Au-Au at 200 GeV [24]. Additionally, hydrodynamical models have been developed to attempt to explain the STAR results without invoking the CMW [40,41]. However, no theoretical modeling or calculations at all, regardless of mechanism, are available for Pb-Pb collisions at $\sqrt{s_{NN}} = 2.76$ TeV.

D. Differential correlator results as a function of $\Delta\eta$

As discussed above, the definition of the three particle differential correlator includes $\langle q_3\rangle_1$, the mean charge of the third particle when evaluated with a selection on q_1. The quantity $\langle q_3\rangle_1 - \langle q_3\rangle$ is shown as a function of $\Delta\eta = \eta_1 - \eta_3$ in Fig. 8. The measurements are performed as a function of $|\Delta\eta|$ and shown as a function of $\Delta\eta$ with the points reflected about $\Delta\eta = 0$. This conditional mean of q_3 depends significantly on $\Delta\eta$ and has the opposite sign when q_1 is flipped. The effect is most pronounced for $\Delta\eta \approx 0$ and weakest when $\Delta\eta$ is large. When the first particle is negative, the third particle has a slightly positive mean charge, and when the first particle is positive, the third particle has a slightly negative mean charge. Note that the quantity $\langle q_3\rangle_1 - \langle q_3\rangle$ is proportional to the charge balance function [33] and as such reflects the charge correlation length.

Figure 9 shows the three-particle correlator for the second harmonic as a function of $\Delta\eta$. The correlator exhibits a rather nontrivial dependence on $\Delta\eta$: a peak with a "typical hadronic width" of about 0.5–1 units of rapidity and a possible change of the sign at about $\Delta\eta \approx 1$ (note, however, these points are consistent with zero within the systematic uncertainties). Both of those features qualitatively agree with possible background contribution from local charge conservation combined with strong radial and elliptic flow [33]. Unfortunately there exist no predictions for this observable from the CMW.

The three-particle correlator for the third and fourth harmonics as a function of $\Delta\eta$ is shown in Fig. 10. The strength of the correlations is significantly reduced, by a factor about 3 in the case of the third harmonic and at least a factor of 5 for the fourth harmonic. The fourth harmonic correlator is consistent with zero within errors. Neglecting flow fluctuations, the CMW expectations for higher harmonics correlators would be zero; unfortunately there are no reliable calculations of the effect of flow fluctuations. The (background) contribution due to the local charge conservation should roughly scale with the magnitude of the flow [33] and is qualitatively consistent with the experimental results. More detailed calculations in both scenarios, as well as more precise data, are obviously needed for a more definitive conclusion.

V. SUMMARY AND OUTLOOK

Novel three-particle correlators have been employed in an experimental search for the CMW. Results have been shown for the second, third, and fourth harmonic for the integrated correlator of the charge-dependent flow as a function of centrality and the differential correlator as a function of pseudorapidity separation. A clear dependence of the positive

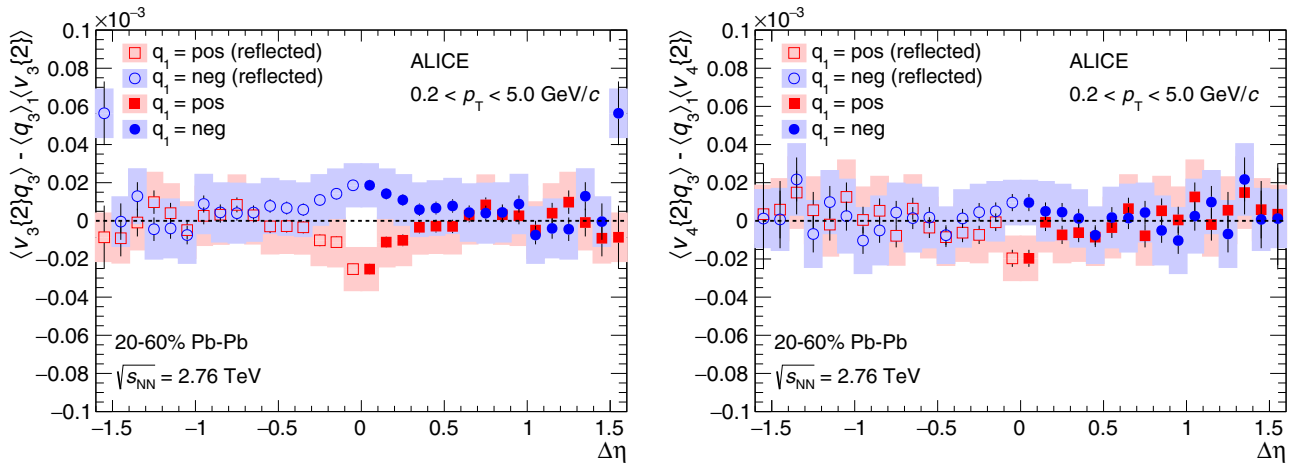

FIG. 10. Three-particle correlator for the third (left panel) and fourth (right panel) harmonics, for positive (red squares) and negative (blue circles) particles. Statistical (systematic) uncertainties are indicated by vertical bars (shaded boxes).

and negative particle anisotropic flow on the event charge asymmetry is presented for different centralities in Pb-Pb collisions. The slopes of this dependence, determined by two different methods, are consistent and qualitatively agree with the expectations for CMW, as well as similar to those measured by the STAR Collaboration at the top Relativistic Heavy Ion Collider (RHIC) energy. The observed nonzero signal in higher harmonics correlations indicates a possible strong background contribution, likely from LCC in combination with strong radial and anisotropic flow. We also have presented results on the differential correlator, which is more sensitive to the detail of the underlying physics and helps to discriminate between the CMW scenario and the background effects. The second harmonic results show a fairly large correlation, and the strength of the correlation strongly decreases with increasing harmonic number. Further input from theory is needed to give detailed constraints on the magnitude and range of background vs CMW correlations.

LHC Run 2 will include Pb-Pb collisions at $\sqrt{s_{NN}} = 5.02$ TeV and will offer substantially higher integrated luminosity, which will largely improve statistical precision of these measurements, and may also help reduce some of the systematic uncertainties. One of the chief benefits of increased statistical precision would be the possibility to evaluate the three-particle correlator with identified particles. The species of both particle 1 and 3 is of potential interest. The different collision energy affects both the peak strength (which increases) and the lifetime (which decreases) of the magnetic field induced in the collision, which provides additional information. For that reason, an analysis of this correlator at lower collisions energies, for example at RHIC, would provide important additional insights.

ACKNOWLEDGMENTS

The ALICE Collaboration would like to thank all its engineers and technicians for their invaluable contributions to the construction of the experiment and the CERN accelerator teams for the outstanding performance of the LHC complex. The ALICE Collaboration gratefully acknowledges the resources and support provided by all Grid centres and the Worldwide LHC Computing Grid (WLCG) Collaboration. The ALICE Collaboration acknowledges the following funding agencies for their support in building and running the ALICE detector: State Committee of Science, World Federation of Scientists (WFS), and Swiss Fonds Kidagan, Armenia; Conselho Nacional de Desenvolvimento Científico e Tecnológico (CNPq), Financiadora de Estudos e Projetos (FINEP), Fundação de Amparo à Pesquisa do Estado de São Paulo (FAPESP); National Natural Science Foundation of China (NSFC), the Chinese Ministry of Education (CMOE), and the Ministry of Science and Technology of China (MSTC); Ministry of Education and Youth of the Czech Republic; Danish Natural Science Research Council, the Carlsberg Foundation, and the Danish National Research Foundation; The European Research Council under the European Community's Seventh Framework Programme; Helsinki Institute of Physics and the Academy of Finland; French CNRS-IN2P3, the "Region Pays de Loire", "Region Alsace", "Region Auvergne", and CEA, France; German Bundesministerium fur Bildung, Wissenschaft, Forschung und Technologie (BMBF) and the Helmholtz Association; General Secretariat for Research and Technology, Ministry of Development, Greece; National Research, Development and Innovation Office (NKFIH), Hungary; Department of Atomic Energy and Department of Science and Technology of the Government of India; Istituto Nazionale di Fisica Nucleare (INFN) and Centro Fermi - Museo Storico della Fisica e Centro Studi e Ricerche "Enrico Fermi", Italy; Japan Society for the Promotion of Science (JSPS) KAKENHI and MEXT, Japan; Joint Institute for Nuclear Research, Dubna; National Research Foundation of Korea (NRF); Consejo Nacional de Cienca y Tecnologia (CONACYT), Dirección General de Asuntos del Personal Académico (DGAPA), México, Amerique Latine Formation Academique - European Commission (ALFA-EC), and the EPLANET Program (European Particle Physics Latin American Network); Stichting voor Fundamenteel Onderzoek der Materie (FOM) and the Nederlandse Organisatie voor Wetenschappelijk Onderzoek (NWO), Netherlands; Research Council of Norway (NFR); National Science Centre, Poland; Ministry of National Education/Institute for Atomic Physics and National Council of Scientific Research in Higher Education (CNCSI-UEFISCDI), Romania; Ministry of Education and Science of Russian Federation, Russian Academy of Sciences, Russian Federal Agency of Atomic Energy, Russian Federal Agency for Science and Innovations, and The Russian Foundation for Basic Research; Ministry of Education of Slovakia; Department of Science and Technology, South Africa; Centro de Investigaciones Energeticas, Medioambientales y Tecnologicas (CIEMAT), E-Infrastructure shared between Europe and Latin America (EELA), Ministerio de Economía y Competitividad (MINECO) of Spain, Xunta de Galicia (Consellería de Educación), Centro de Aplicaciones TecnolÃ³gicas y Desarrollo Nuclear (CEADEN), Cubaenergía, Cuba, and IAEA (International Atomic Energy Agency); Swedish Research Council (VR) and Knut & Alice Wallenberg Foundation (KAW); Ukraine Ministry of Education and Science; United Kingdom Science and Technology Facilities Council (STFC); The United States Department of Energy, the United States National Science Foundation, the State of Texas, and the State of Ohio; Ministry of Science, Education and Sports of Croatia and Unity through Knowledge Fund, Croatia; Council of Scientific and Industrial Research (CSIR), New Delhi, India; Pontificia Universidad Católica del Perú.

[1] T. Lee and C.-N. Yang, Question of Parity Conservation in Weak Interactions, Phys. Rev. **104**, 254 (1956).

[2] C. Wu, E. Ambler, R. Hayward, D. Hoppes, and R. Hudson, Experimental Test of Parity Conservation in Beta Decay, Phys. Rev. **105**, 1413 (1957).

[3] R. Garwin, L. Lederman, and M. Weinrich, Observations of the Failure of Conservation of Parity and Charge Conjugation in Meson Decays: The Magnetic Moment of the Free Muon, Phys. Rev. **105**, 1415 (1957).

[4] J. Smith, E. Purcell, and N. Ramsey, Experimental limit to the electric dipole moment of the neutron, Phys. Rev. **108**, 120 (1957).
[5] C. Baker, D. Doyle, P. Geltenbort, K. Green, M. van der Grinten *et al.*, An Improved Experimental Limit on the Electric Dipole Moment of the Neutron, Phys. Rev. Lett. **97**, 131801 (2006).
[6] T. Lee, A theory of spontaneous T violation, Phys. Rev. D **8**, 1226 (1973).
[7] T. Lee and G. Wick, Vacuum stability and vacuum excitation in a spin-0 field theory, Phys. Rev. D **9**, 2291 (1974).
[8] P. Morley and I. Schmidt, Strong P, CP, T violations in heavy ion collisions, Z. Phys. C **26**, 627 (1985).
[9] D. Kharzeev, R. D. Pisarski, and M. H. Tytgat, Possibility of Spontaneous Parity Violation in Hot QCD, Phys. Rev. Lett. **81**, 512 (1998).
[10] D. Kharzeev, R. D. Pisarski, and M. H. Tytgat, Parity odd bubbles in hot QCD, arXiv:hep-ph/9808366.
[11] D. Kharzeev, R. D. Pisarski, and M. H. Tytgat, Aspects of parity, CP, and time reversal violation in hot QCD, arXiv:hep-ph/0012012.
[12] S. A. Voloshin, Discussing the possibility of observation of parity violation in heavy ion collisions, Phys. Rev. C **62**, 044901 (2000).
[13] D. Kharzeev, Parity violation in hot QCD: Why it can happen, and how to look for it, Phys. Lett. B **633**, 260 (2006).
[14] S. A. Voloshin, Parity violation in hot QCD: How to detect it, Phys. Rev. C **70**, 057901 (2004).
[15] S. Voloshin and Y. Zhang, Flow study in relativistic nuclear collisions by Fourier expansion of azimuthal particle distributions, Z. Phys. C **70**, 665 (1996).
[16] V. Skokov, A. Y. Illarionov, and V. Toneev, Estimate of the magnetic field strength in heavy-ion collisions, Int. J. Mod. Phys. A **24**, 5925 (2009).
[17] Y. Zhong, C.-B. Yang, X. Cai, and S.-Q. Feng, A systematic study of magnetic field in relativistic heavy-ion collisions in the RHIC and LHC energy regions, Adv. High Energy Phys. **2014**, 193039 (2014).
[18] K. Tuchin, Particle production in strong electromagnetic fields in relativistic heavy-ion collisions, Adv. High Energy Phys. **2013**, 490495 (2013).
[19] L. McLerran and V. Skokov, Comments about the electromagnetic field in heavy-ion collisions, Nucl. Phys. A **929**, 184 (2014).
[20] K. Fukushima, D. Kharzeev, and H. J. Warringa, The chiral magnetic effect, Phys. Rev. D **78**, 074033 (2008).
[21] D. T. Son and P. Surowka, Hydrodynamics with Triangle Anomalies, Phys. Rev. Lett. **103**, 191601 (2009).
[22] D. Kharzeev and H.-U. Yee, Chiral magnetic wave, Phys. Rev. D **83**, 085007 (2011).
[23] Y. Burnier, D. Kharzeev, J. Liao, and H.-U. Yee, Chiral Magnetic Wave at Finite Baryon Density and the Electric Quadrupole Moment of Quark-Gluon Plasma in Heavy Ion Collisions, Phys. Rev. Lett. **107**, 052303 (2011).
[24] Y. Burnier, D. Kharzeev, J. Liao, and H.-U. Yee, From the chiral magnetic wave to the charge dependence of elliptic flow, in RBRC Workshop Proceedings, Volume 110 (2012), arXiv:1208.2537.
[25] B. Abelev *et al.* (ALICE Collaboration), Multiparticle azimuthal correlations in p-Pb and Pb-Pb collisions at the LHC, Phys. Rev. C **90**, 054901 (2014).
[26] J. Bjorken, Highly relativistic nucleus-nucleus collisions: The central rapidity region, Phys. Rev. D **27**, 140 (1983).
[27] B. Abelev *et al.* (ALICE Collaboration), Charge Separation Relative to the Reaction Plane in Pb-Pb Collisions at $\sqrt{s_{NN}} =$ 2.76 TeV, Phys. Rev. Lett. **110**, 012301 (2013).
[28] S. F. Taghavi and U. A. Wiedemann, The chiral magnetic wave in an expanding QCD fluid, Phys. Rev. C **91**, 024902 (2015).
[29] H.-U. Yee and Y. Yin, Realistic implementation of chiral magnetic wave in heavy ion collisions, Phys. Rev. C **89**, 044909 (2014).
[30] L. Adamczyk *et al.* (STAR Collaboration), Observation of Charge Asymmetry Dependence of Pion Elliptic Flow and the Possible Chiral Magnetic Wave in Heavy-Ion Collisions, Phys. Rev. Lett. **114**, 252302 (2015).
[31] G. Wang (STAR Collaboration), Search for chiral magnetic effects in high-energy nuclear collisions, Nucl. Phys. A **904-905**, 248c (2013).
[32] H. Ke (STAR Collaboration), Charge asymmetry dependency of π^+/π^- elliptic flow in Au + Au collisions at $\sqrt{s_{NN}} = 200$ GeV, J. Phys. Conf. Ser. **389**, 012035 (2012).
[33] S. A. Voloshin and R. Belmont, Measuring and interpreting charge dependent anisotropic flow, Nucl. Phys. A **931**, 992 (2014).
[34] R. Belmont (ALICE Collaboration), Charge-dependent anisotropic flow studies and the search for the chiral magnetic wave in ALICE, Nucl. Phys. A **931**, 981 (2014).
[35] R. Brun, F. Carminati, and S. Giani, GEANT Detector Description and Simulation Tool, CERN Program Library Long Writeup W5013, 1994 (unpublished).
[36] K. Aamodt *et al.* (ALICE Collaboration), The ALICE experiment at the CERN LHC, J. Instrum. **3**, S08002 (2008).
[37] B. Abelev *et al.* (ALICE Collaboration), Performance of the ALICE experiment at the CERN LHC, Int. J. Mod. Phys. A **29**, 1430044 (2014).
[38] X.-N. Wang and M. Gyulassy, HIJING: A Monte Carlo model for multiple jet production in pp, pA, and AA collisions, Phys. Rev. D **44**, 3501 (1991).
[39] K. Aamodt *et al.* (ALICE Collaboration), Centrality Dependence of the Charged-Particle Multiplicity Density at Midrapidity in Pb-Pb Collisions at $\sqrt{s_{NN}} = 2.76$ TeV, Phys. Rev. Lett. **106**, 032301 (2011)
[40] A. Bzdak and P. Bozek, Contributions to the event-by-event charge asymmetry dependence for the elliptic flow of pi^+ and pi^- in heavy-ion collisions, Phys. Lett. B **726**, 239 (2013)
[41] Y. Hatta, A. Monnai, and B.-W. Xiao, Elliptic flow difference of charged pions in heavy-ion collisions, Nucl. Phys. A **947**, 155 (2016).

J. Adam,[40] D. Adamová,[84] M. M. Aggarwal,[88] G. Aglieri Rinella,[36] M. Agnello,[110] N. Agrawal,[48] Z. Ahammed,[132] S. U. Ahn,[68] S. Aiola,[136,†] A. Akindinov,[58] S. N. Alam,[132] D. Aleksandrov,[80] B. Alessandro,[110] D. Alexandre,[101] R. Alfaro Molina,[64]

A. Alici,[104,12] A. Alkin,[3] J. R. M. Almaraz,[119] J. Alme,[38] T. Alt,[43] S. Altinpinar,[18] I. Altsybeev,[131] C. Alves Garcia Prado,[120] C. Andrei,[78] A. Andronic,[97] V. Anguelov,[94] J. Anielski,[54] T. Antičić,[98] F. Antinori,[107] P. Antonioli,[104] L. Aphecetche,[113] H. Appelshäuser,[53] S. Arcelli,[28] R. Arnaldi,[110] O. W. Arnold,[37,93] I. C. Arsene,[22] M. Arslandok,[53] B. Audurier,[113] A. Augustinus,[36] R. Averbeck,[97] M. D. Azmi,[19] A. Badalà,[106] Y. W. Baek,[67] S. Bagnasco,[110] R. Bailhache,[53] R. Bala,[91] S. Balasubramanian,[136] A. Baldisseri,[15] R. C. Baral,[61] A. M. Barbano,[27] R. Barbera,[29] F. Barile,[33] G. G. Barnaföldi,[135,*] L. S. Barnby,[101] V. Barret,[70] P. Bartalini,[7] K. Barth,[36] J. Bartke,[117] E. Bartsch,[53] M. Basile,[28] N. Bastid,[70] S. Basu,[132] B. Bathen,[54] G. Batigne,[113] A. Batista Camejo,[70] B. Batyunya,[66] P. C. Batzing,[22] I. G. Bearden,[81] H. Beck,[53] C. Bedda,[110] N. K. Behera,[50] I. Belikov,[55] F. Bellini,[28] H. Bello Martinez,[2] R. Bellwied,[122] R. Belmont,[134] E. Belmont-Moreno,[64] V. Belyaev,[75] P. Benacek,[84] G. Bencedi,[135] S. Beole,[27] I. Berceanu,[78] A. Bercuci,[78] Y. Berdnikov,[86] D. Berenyi,[135] R. A. Bertens,[57] D. Berzano,[36] L. Betev,[36] A. Bhasin,[91] I. R. Bhat,[91] A. K. Bhati,[88] B. Bhattacharjee,[45] J. Bhom,[128] L. Bianchi,[122] N. Bianchi,[72] C. Bianchin,[134,57] J. Bielčík,[40] J. Bielčíková,[84] A. Bilandzic,[81,37,93] G. Biro,[135] R. Biswas,[4] S. Biswas,[79] S. Bjelogrlic,[57] J. T. Blair,[118] D. Blau,[80] C. Blume,[53] F. Bock,[74,94] A. Bogdanov,[75] H. Bøggild,[81] L. Boldizsár,[135] M. Bombara,[41] J. Book,[53] H. Borel,[15] A. Borissov,[96] M. Borri,[83,124] F. Bossú,[65] E. Botta,[27] C. Bourjau,[81] P. Braun-Munzinger,[97] M. Bregant,[120] T. Breitner,[52] T. A. Broker,[53] T. A. Browning,[95] M. Broz,[40] E. J. Brucken,[46] E. Bruna,[110] G. E. Bruno,[33] D. Budnikov,[99] H. Buesching,[53] S. Bufalino,[27,36] P. Buncic,[36] O. Busch,[94,128] Z. Buthelezi,[65] J. B. Butt,[16] J. T. Buxton,[20] D. Caffarri,[36] X. Cai,[7] H. Caines,[136] L. Calero Diaz,[72] A. Caliva,[57] E. Calvo Villar,[102] P. Camerini,[26] F. Carena,[36] W. Carena,[36] F. Carnesecchi,[28] J. Castillo Castellanos,[15] A. J. Castro,[125] E. A. R. Casula,[25] C. Ceballos Sanchez,[9] P. Cerello,[110] J. Cerkala,[115] B. Chang,[123] S. Chapeland,[36] M. Chartier,[124] J. L. Charvet,[15] S. Chattopadhyay,[132] S. Chattopadhyay,[100] A. Chauvin,[93,37] V. Chelnokov,[3] M. Cherney,[87] C. Cheshkov,[130] B. Cheynis,[130] V. Chibante Barroso,[36] D. D. Chinellato,[121] S. Cho,[50] P. Chochula,[36] K. Choi,[96] M. Chojnacki,[81] S. Choudhury,[132] P. Christakoglou,[82] C. H. Christensen,[81] P. Christiansen,[34] T. Chujo,[128] S. U. Chung,[96] C. Cicalo,[105] L. Cifarelli,[12,28] F. Cindolo,[104] J. Cleymans,[90] F. Colamaria,[33] D. Colella,[59,36] A. Collu,[74,25] M. Colocci,[28] G. Conesa Balbastre,[71] Z. Conesa del Valle,[51] M. E. Connors,[136,†] J. G. Contreras,[40] T. M. Cormier,[85] Y. Corrales Morales,[110] I. Cortés Maldonado,[2] P. Cortese,[32] M. R. Cosentino,[120] F. Costa,[36] P. Crochet,[70] R. Cruz Albino,[11] E. Cuautle,[63] L. Cunqueiro,[54,36] T. Dahms,[93,37] A. Dainese,[107] A. Danu,[62] D. Das,[100] I. Das,[51,100] S. Das,[4] A. Dash,[121,79] S. Dash,[48] S. De,[120] A. De Caro,[31,12] G. de Cataldo,[103] C. de Conti,[120] J. de Cuveland,[43] A. De Falco,[25] D. De Gruttola,[12,31] N. De Marco,[110] S. De Pasquale,[31] A. Deisting,[97,94] A. Deloff,[77] E. Dénes,[135,*] C. Deplano,[82] P. Dhankher,[48] D. Di Bari,[33] A. Di Mauro,[36] P. Di Nezza,[72] M. A. Diaz Corchero,[10] T. Dietel,[90] P. Dillenseger,[53] R. Divià,[36] Ø. Djuvsland,[18] A. Dobrin,[82,57] D. Domenicis Gimenez,[120] B. Dönigus,[53] O. Dordic,[22] T. Drozhzhova,[53] A. K. Dubey,[132] A. Dubla,[57] L. Ducroux,[130] P. Dupieux,[70] R. J. Ehlers,[136] D. Elia,[103] E. Endress,[102] H. Engel,[52] E. Epple,[136] B. Erazmus,[113] I. Erdemir,[53] F. Erhardt,[129] B. Espagnon,[51] M. Estienne,[113] S. Esumi,[128] J. Eum,[96] D. Evans,[101] S. Evdokimov,[111] G. Eyyubova,[40] L. Fabbietti,[93,37] D. Fabris,[107] J. Faivre,[71] A. Fantoni,[72] M. Fasel,[74] L. Feldkamp,[54] A. Feliciello,[110] G. Feofilov,[131] J. Ferencei,[84] A. Fernández Téllez,[2] E. G. Ferreiro,[17] A. Ferretti,[27] A. Festanti,[30] V. J. G. Feuillard,[15,70] J. Figiel,[117] M. A. S. Figueredo,[124,120] S. Filchagin,[99] D. Finogeev,[56] F. M. Fionda,[25] E. M. Fiore,[33] M. G. Fleck,[94] M. Floris,[36] S. Foertsch,[65] P. Foka,[97] S. Fokin,[80] E. Fragiacomo,[109] A. Francescon,[36,30] U. Frankenfeld,[97] G. G. Fronze,[27] U. Fuchs,[36] C. Furget,[71] A. Furs,[56] M. Fusco Girard,[31] J. J. Gaardhøje,[81] M. Gagliardi,[27] A. M. Gago,[102] M. Gallio,[27] D. R. Gangadharan,[74] P. Ganoti,[89] C. Gao,[7] C. Garabatos,[97] E. Garcia-Solis,[13] C. Gargiulo,[36] P. Gasik,[93,37] E. F. Gauger,[118] M. Germain,[113] A. Gheata,[36] M. Gheata,[36,62] P. Ghosh,[132] S. K. Ghosh,[4] P. Gianotti,[72] P. Giubellino,[110,36] P. Giubilato,[30] E. Gladysz-Dziadus,[117] P. Glässel,[94] D. M. Goméz Coral,[64] A. Gomez Ramirez,[52] V. Gonzalez,[10] P. González-Zamora,[10] S. Gorbunov,[43] L. Görlich,[117] S. Gotovac,[116] V. Grabski,[64] O. A. Grachov,[136] L. K. Graczykowski,[133] K. L. Graham,[101] A. Grelli,[57] A. Grigoras,[36] C. Grigoras,[36] V. Grigoriev,[75] A. Grigoryan,[1] S. Grigoryan,[66] B. Grinyov,[3] N. Grion,[109] J. M. Gronefeld,[97] J. F. Grosse-Oetringhaus,[36] J.-Y. Grossiord,[130] R. Grosso,[97] F. Guber,[56] R. Guernane,[71] B. Guerzoni,[28] K. Gulbrandsen,[81] T. Gunji,[127] A. Gupta,[91] R. Gupta,[91] R. Haake,[54] Ø. Haaland,[18] C. Hadjidakis,[51] M. Haiduc,[62] H. Hamagaki,[127] G. Hamar,[135] J. C. Hamon,[55] J. W. Harris,[136] A. Harton,[13] D. Hatzifotiadou,[104] S. Hayashi,[127] S. T. Heckel,[53] H. Helstrup,[38] A. Herghelegiu,[78] G. Herrera Corral,[11] B. A. Hess,[35] K. F. Hetland,[38] H. Hillemanns,[36] B. Hippolyte,[55] D. Horak,[40] R. Hosokawa,[128] P. Hristov,[36] M. Huang,[18] T. J. Humanic,[20] N. Hussain,[45] T. Hussain,[19] D. Hutter,[43] D. S. Hwang,[21] R. Ilkaev,[99] M. Inaba,[128] E. Incani,[25] M. Ippolitov,[75,80] M. Irfan,[19] M. Ivanov,[97] V. Ivanov,[86] V. Izucheev,[111] N. Jacazio,[28] P. M. Jacobs,[74] M. B. Jadhav,[48] S. Jadlovska,[115] J. Jadlovsky,[115,59] C. Jahnke,[120] M. J. Jakubowska,[133] H. J. Jang,[68] M. A. Janik,[133] P. H. S. Y. Jayarathna,[122] C. Jena,[30] S. Jena,[122] R. T. Jimenez Bustamante,[97] P. G. Jones,[101] H. Jung,[44] A. Jusko,[101] P. Kalinak,[59] A. Kalweit,[36] J. Kamin,[53] J. H. Kang,[137] V. Kaplin,[75] S. Kar,[132] A. Karasu Uysal,[69] O. Karavichev,[56] T. Karavicheva,[56] L. Karayan,[97,94] E. Karpechev,[56] U. Kebschull,[52] R. Keidel,[138] D. L. D. Keijdener,[57] M. Keil,[36] M. Mohisin Khan,[19,‡] P. Khan,[100] S. A. Khan,[132] A. Khanzadeev,[86] Y. Kharlov,[111] B. Kileng,[38] D. W. Kim,[44] D. J. Kim,[123] D. Kim,[137] H. Kim,[137] J. S. Kim,[44] M. Kim,[44] M. Kim,[137] S. Kim,[21] T. Kim,[137] S. Kirsch,[43] I. Kisel,[43] S. Kiselev,[58] A. Kisiel,[133] G. Kiss,[135] J. L. Klay,[6] C. Klein,[53] J. Klein,[36] C. Klein-Bösing,[54] S. Klewin,[94] A. Kluge,[36] M. L. Knichel,[94] A. G. Knospe,[118,122] C. Kobdaj,[114] M. Kofarago,[36] T. Kollegger,[97] A. Kolojvari,[131] V. Kondratiev,[131] N. Kondratyeva,[75] E. Kondratyuk,[111] A. Konevskikh,[56] M. Kopcik,[115] M. Kour,[91] C. Kouzinopoulos,[36] O. Kovalenko,[77] V. Kovalenko,[131] M. Kowalski,[117] G. Koyithatta Meethaleveedu,[48] I. Králik,[59] A. Kravčáková,[41] M. Kretz,[43] M. Krivda,[59,101] F. Krizek,[84] E. Kryshen,[86,36] M. Krzewicki,[43] A. M. Kubera,[20] V. Kučera,[84] C. Kuhn,[55] P. G. Kuijer,[82] A. Kumar,[91] J. Kumar,[48] L. Kumar,[88] S. Kumar,[48] P. Kurashvili,[77] A. Kurepin,[56] A. B. Kurepin,[56] A. Kuryakin,[99] M. J. Kweon,[50] Y. Kwon,[137] S. L. La Pointe,[110] P. La Rocca,[29] P. Ladron de Guevara,[11] C. Lagana Fernandes,[120]

I. Lakomov,[36] R. Langoy,[42] C. Lara,[52] A. Lardeux,[15] A. Lattuca,[27] E. Laudi,[36] R. Lea,[26] L. Leardini,[94] G. R. Lee,[101] S. Lee,[137] F. Lehas,[82] R. C. Lemmon,[83] V. Lenti,[103] E. Leogrande,[57] I. León Monzón,[119] H. León Vargas,[64] M. Leoncino,[27] P. Lévai,[135] S. Li,[7,70] X. Li,[14] J. Lien,[42] R. Lietava,[101] S. Lindal,[22] V. Lindenstruth,[43] C. Lippmann,[97] M. A. Lisa,[20] H. M. Ljunggren,[34] D. F. Lodato,[57] P. I. Loenne,[18] V. Loginov,[75] C. Loizides,[74] X. Lopez,[70] E. López Torres,[9] A. Lowe,[135] P. Luettig,[53] M. Lunardon,[30] G. Luparello,[26] T. H. Lutz,[136] A. Maevskaya,[56] M. Mager,[36] S. Mahajan,[91] S. M. Mahmood,[22] A. Maire,[55] R. D. Majka,[136] M. Malaev,[86] I. Maldonado Cervantes,[63] L. Malinina,[66,§] D. Mal'Kevich,[58] P. Malzacher,[97] A. Mamonov,[99] V. Manko,[80] F. Manso,[70] V. Manzari,[36,103] M. Marchisone,[27,65,126] J. Mareš,[60] G. V. Margagliotti,[26] A. Margotti,[104] J. Margutti,[57] A. Marín,[97] C. Markert,[118] M. Marquard,[53] N. A. Martin,[97] J. Martin Blanco,[113] P. Martinengo,[36] M. I. Martínez,[2] G. Martínez García,[113] M. Martinez Pedreira,[36] A. Mas,[120] S. Masciocchi,[97] M. Masera,[27] A. Masoni,[105] L. Massacrier,[113] A. Mastroserio,[33] A. Matyja,[117] C. Mayer,[117,36] J. Mazer,[125] M. A. Mazzoni,[108] D. Mcdonald,[122] F. Meddi,[24] Y. Melikyan,[75] A. Menchaca-Rocha,[64] E. Meninno,[31] J. Mercado Pérez,[94] M. Meres,[39] Y. Miake,[128] M. M. Mieskolainen,[46] K. Mikhaylov,[66,58] L. Milano,[74,36] J. Milosevic,[22] L. M. Minervini,[103,23] A. Mischke,[57] A. N. Mishra,[49] D. Miśkowiec,[97] J. Mitra,[132] C. M. Mitu,[62] N. Mohammadi,[57] B. Mohanty,[79] L. Molnar,[55,113] L. Montaño Zetina,[11] E. Montes,[10] D. A. Moreira De Godoy,[54,113] L. A. P. Moreno,[2] S. Moretto,[30] A. Morreale,[113] A. Morsch,[36] V. Muccifora,[72] E. Mudnic,[116] D. Mühlheim,[54] S. Muhuri,[132] M. Mukherjee,[132] J. D. Mulligan,[136] M. G. Munhoz,[120] R. H. Munzer,[93,37] H. Murakami,[127] S. Murray,[65] L. Musa,[36] J. Musinsky,[59] B. Naik,[48] R. Nair,[77] B. K. Nandi,[48] R. Nania,[104] E. Nappi,[103] M. U. Naru,[16] H. Natal da Luz,[120] C. Nattrass,[125] S. R. Navarro,[2] K. Nayak,[79] R. Nayak,[48] T. K. Nayak,[132] S. Nazarenko,[99] A. Nedosekin,[58] L. Nellen,[63] F. Ng,[122] M. Nicassio,[97] M. Niculescu,[62] J. Niedziela,[36] B. S. Nielsen,[81] S. Nikolaev,[80] S. Nikulin,[80] V. Nikulin,[86] F. Noferini,[104,12] P. Nomokonov,[66] G. Nooren,[57] J. C. C. Noris,[2] J. Norman,[124] A. Nyanin,[80] J. Nystrand,[18] H. Oeschler,[94] S. Oh,[136] S. K. Oh,[67] A. Ohlson,[36] A. Okatan,[69] T. Okubo,[47] L. Olah,[135] J. Oleniacz,[133] A. C. Oliveira Da Silva,[120] M. H. Oliver,[136] J. Onderwaater,[97] C. Oppedisano,[110] R. Orava,[46] A. Ortiz Velasquez,[63] A. Oskarsson,[34] J. Otwinowski,[117] K. Oyama,[94,76] M. Ozdemir,[53] Y. Pachmayer,[94] P. Pagano,[31] G. Paić,[63] S. K. Pal,[132] J. Pan,[134] A. K. Pandey,[48] P. Papcun,[115] V. Papikyan,[1] G. S. Pappalardo,[106] P. Pareek,[49] W. J. Park,[97] S. Parmar,[88] A. Passfeld,[54] V. Paticchio,[103] R. N. Patra,[132] B. Paul,[110,100] H. Pei,[7] T. Peitzmann,[57] H. Pereira Da Costa,[15] D. Peresunko,[80,75] C. E. Pérez Lara,[82] E. Perez Lezama,[53] V. Peskov,[53] Y. Pestov,[5] V. Petráček,[40] V. Petrov,[111] M. Petrovici,[78] C. Petta,[29] S. Piano,[109] M. Pikna,[39] P. Pillot,[113] L. O. D. L. Pimentel,[81] O. Pinazza,[104,36] L. Pinsky,[122] D. B. Piyarathna,[122] M. Płoskoń,[74] M. Planinic,[129] J. Pluta,[133] S. Pochybova,[135] P. L. M. Podesta-Lerma,[119] M. G. Poghosyan,[85,87] B. Polichtchouk,[111] N. Poljak,[129] W. Poonsawat,[114] A. Pop,[78] S. Porteboeuf-Houssais,[70] J. Porter,[74] J. Pospisil,[84] S. K. Prasad,[4] R. Preghenella,[104,36] F. Prino,[110] C. A. Pruneau,[134] I. Pshenichnov,[56] M. Puccio,[27] G. Puddu,[25] P. Pujahari,[134] V. Punin,[99] J. Putschke,[134] H. Qvigstad,[22] A. Rachevski,[109] S. Raha,[4] S. Rajput,[91] J. Rak,[123] A. Rakotozafindrabe,[15] L. Ramello,[32] F. Rami,[55] R. Raniwala,[92] S. Raniwala,[92] S. S. Räsänen,[46] B. T. Rascanu,[53] D. Rathee,[88] K. F. Read,[85,125] K. Redlich,[77] R. J. Reed,[134] A. Rehman,[18] P. Reichelt,[53] F. Reidt,[94,36] X. Ren,[7] R. Renfordt,[53] A. R. Reolon,[72] A. Reshetin,[56] J.-P. Revol,[12] K. Reygers,[94] V. Riabov,[86] R. A. Ricci,[73] T. Richert,[34] M. Richter,[22] P. Riedler,[36] W. Riegler,[36] F. Riggi,[29] C. Ristea,[62] E. Rocco,[57] M. Rodríguez Cahuantzi,[11,2] A. Rodriguez Manso,[82] K. Røed,[22] E. Rogochaya,[66] D. Rohr,[43] D. Röhrich,[18] R. Romita,[124] F. Ronchetti,[72,36] L. Ronflette,[113] P. Rosnet,[70] A. Rossi,[36,30] F. Roukoutakis,[89] A. Roy,[49] C. Roy,[55] P. Roy,[100] A. J. Rubio Montero,[10] R. Rui,[26] R. Russo,[27] E. Ryabinkin,[80] Y. Ryabov,[86] A. Rybicki,[117] S. Sadovsky,[111] K. Šafařík,[36] B. Sahlmuller,[53] P. Sahoo,[49] R. Sahoo,[49] S. Sahoo,[61] P. K. Sahu,[61] J. Saini,[132] S. Sakai,[72] M. A. Saleh,[134] J. Salzwedel,[20] S. Sambyal,[91] V. Samsonov,[86] L. Šándor,[59] A. Sandoval,[64] M. Sano,[128] D. Sarkar,[132] P. Sarma,[45] E. Scapparone,[104] F. Scarlassara,[30] C. Schiaua,[78] R. Schicker,[94] C. Schmidt,[97] H. R. Schmidt,[35] S. Schuchmann,[53] J. Schukraft,[36] M. Schulc,[40] T. Schuster,[136] Y. Schutz,[36,113] K. Schwarz,[97] K. Schweda,[97] G. Scioli,[28] E. Scomparin,[110] R. Scott,[125] M. Šefčík,[41] J. E. Seger,[87] Y. Sekiguchi,[127] D. Sekihata,[47] I. Selyuzhenkov,[97] K. Senosi,[65] S. Senyukov,[3,36] E. Serradilla,[10,64] A. Sevcenco,[62] A. Shabanov,[56] A. Shabetai,[113] O. Shadura,[3] R. Shahoyan,[36] A. Shangaraev,[111] A. Sharma,[91] M. Sharma,[91] M. Sharma,[91] N. Sharma,[125] K. Shigaki,[47] K. Shtejer,[27,9] Y. Sibiriak,[80] S. Siddhanta,[105] K. M. Sielewicz,[36] T. Siemiarczuk,[77] D. Silvermyr,[34] C. Silvestre,[71] G. Simatovic,[129] G. Simonetti,[36] R. Singaraju,[132] R. Singh,[79] S. Singha,[132,79] V. Singhal,[132] B. C. Sinha,[132] T. Sinha,[100] B. Sitar,[39] M. Sitta,[32] T. B. Skaali,[22] M. Slupecki,[123] N. Smirnov,[136] R. J. M. Snellings,[57] T. W. Snellman,[123] C. Søgaard,[34] J. Song,[96] M. Song,[137] Z. Song,[7] F. Soramel,[30] S. Sorensen,[125] R. D. de Souza,[121] F. Sozzi,[97] M. Spacek,[40] E. Spiriti,[72] I. Sputowska,[117] M. Spyropoulou-Stassinaki,[89] J. Stachel,[94] I. Stan,[62] P. Stankus,[85] G. Stefanek,[77] E. Stenlund,[34] G. Steyn,[65] J. H. Stiller,[94] D. Stocco,[113] P. Strmen,[39] A. A. P. Suaide,[120] T. Sugitate,[47] C. Suire,[51] M. Suleymanov,[16] M. Suljic,[26,*] R. Sultanov,[58] M. Šumbera,[84] A. Szabo,[39] A. Szanto de Toledo,[120,*] I. Szarka,[39] A. Szczepankiewicz,[36] M. Szymanski,[133] U. Tabassam,[16] J. Takahashi,[121] G. J. Tambave,[18] N. Tanaka,[128] M. A. Tangaro,[33] M. Tarhini,[51] M. Tariq,[19] M. G. Tarzila,[78] A. Tauro,[36] G. Tejeda Muñoz,[2] A. Telesca,[36] K. Terasaki,[127] C. Terrevoli,[30] B. Teyssier,[130] J. Thäder,[74] D. Thomas,[118] R. Tieulent,[130] A. R. Timmins,[122] A. Toia,[53] S. Trogolo,[27] G. Trombetta,[33] V. Trubnikov,[3] W. H. Trzaska,[123] T. Tsuji,[127] A. Tumkin,[99] R. Turrisi,[107] T. S. Tveter,[22] K. Ullaland,[18] A. Uras,[130] G. L. Usai,[25] A. Utrobicic,[129] M. Vajzer,[84] M. Vala,[59] L. Valencia Palomo,[70] S. Vallero,[27] J. Van Der Maarel,[57] J. W. Van Hoorne,[36] M. van Leeuwen,[57] T. Vanat,[84] P. Vande Vyvre,[36] D. Varga,[135] A. Vargas,[2] M. Vargyas,[123] R. Varma,[48] M. Vasileiou,[89] A. Vasiliev,[80] A. Vauthier,[71] V. Vechernin,[131] A. M. Veen,[57] M. Veldhoen,[57] A. Velure,[18] M. Venaruzzo,[73] E. Vercellin,[27] S. Vergara Limón,[2] R. Vernet,[8] M. Verweij,[134] L. Vickovic,[116] G. Viesti,[30,*] J. Viinikainen,[123] Z. Vilakazi,[126] O. Villalobos Baillie,[101] A. Villatoro Tello,[2] A. Vinogradov,[80] L. Vinogradov,[131] Y. Vinogradov,[99,*] T. Virgili,[31] V. Vislavicius,[34] Y. P. Viyogi,[132] A. Vodopyanov,[66] M. A. Völkl,[94] K. Voloshin,[58] S. A. Voloshin,[134] G. Volpe,[135] B. von

Haller,[36] I. Vorobyev,[37,93] D. Vranic,[97,36] J. Vrláková,[41] B. Vulpescu,[70] B. Wagner,[18] J. Wagner,[97] H. Wang,[57] M. Wang,[7,113] D. Watanabe,[128] Y. Watanabe,[127] M. Weber,[36,112] S. G. Weber,[97] D. F. Weiser,[94] J. P. Wessels,[54] U. Westerhoff,[54] A. M. Whitehead,[90] J. Wiechula,[35] J. Wikne,[22] M. Wilde,[54] G. Wilk,[77] J. Wilkinson,[94] M. C. S. Williams,[104] B. Windelband,[94] M. Winn,[94] C. G. Yaldo,[134] H. Yang,[57] P. Yang,[7] S. Yano,[47] C. Yasar,[69] Z. Yin,[7] H. Yokoyama,[128] I.-K. Yoo,[96] J. H. Yoon,[50] V. Yurchenko,[3] I. Yushmanov,[80] A. Zaborowska,[133] V. Zaccolo,[81] A. Zaman,[16] C. Zampolli,[104] H. J. C. Zanoli,[120] S. Zaporozhets,[66] N. Zardoshti,[101] A. Zarochentsev,[131] P. Závada,[60] N. Zaviyalov,[99] H. Zbroszczyk,[133] I. S. Zgura,[62] M. Zhalov,[86] H. Zhang,[18] X. Zhang,[74] Y. Zhang,[7] C. Zhang,[57] Z. Zhang,[7] C. Zhao,[22] N. Zhigareva,[58] D. Zhou,[7] Y. Zhou,[81] Z. Zhou,[18] H. Zhu,[18] J. Zhu,[113,7] A. Zichichi,[28,12] A. Zimmermann,[94] M. B. Zimmermann,[36,54] G. Zinovjev,[3] and M. Zyzak[43]

(ALICE Collaboration)

[1]*A.I. Alikhanyan National Science Laboratory (Yerevan Physics Institute) Foundation, Yerevan, Armenia*
[2]*Benemérita Universidad Autónoma de Puebla, Puebla, Mexico*
[3]*Bogolyubov Institute for Theoretical Physics, Kiev, Ukraine*
[4]*Bose Institute, Department of Physics and Centre for Astroparticle Physics and Space Science (CAPSS), Kolkata, India*
[5]*Budker Institute for Nuclear Physics, Novosibirsk, Russia*
[6]*California Polytechnic State University, San Luis Obispo, California, USA*
[7]*Central China Normal University, Wuhan, China*
[8]*Centre de Calcul de l'IN2P3, Villeurbanne, France*
[9]*Centro de Aplicaciones Tecnológicas y Desarrollo Nuclear (CEADEN), Havana, Cuba*
[10]*Centro de Investigaciones Energéticas Medioambientales y Tecnológicas (CIEMAT), Madrid, Spain*
[11]*Centro de Investigación y de Estudios Avanzados (CINVESTAV), Mexico City and Mérida, Mexico*
[12]*Centro Fermi - Museo Storico della Fisica e Centro Studi e Ricerche "Enrico Fermi", Rome, Italy*
[13]*Chicago State University, Chicago, Illinois, USA*
[14]*China Institute of Atomic Energy, Beijing, China*
[15]*Commissariat à l'Energie Atomique, IRFU, Saclay, France*
[16]*COMSATS Institute of Information Technology (CIIT), Islamabad, Pakistan*
[17]*Departamento de Física de Partículas and IGFAE, Universidad de Santiago de Compostela, Santiago de Compostela, Spain*
[18]*Department of Physics and Technology, University of Bergen, Bergen, Norway*
[19]*Department of Physics, Aligarh Muslim University, Aligarh, India*
[20]*Department of Physics, Ohio State University, Columbus, Ohio, USA*
[21]*Department of Physics, Sejong University, Seoul, South Korea*
[22]*Department of Physics, University of Oslo, Oslo, Norway*
[23]*Dipartimento di Elettrotecnica ed Elettronica del Politecnico, Bari, Italy*
[24]*Dipartimento di Fisica dell'Università 'La Sapienza' and Sezione INFN Rome, Italy*
[25]*Dipartimento di Fisica dell'Università and Sezione INFN, Cagliari, Italy*
[26]*Dipartimento di Fisica dell'Università and Sezione INFN, Trieste, Italy*
[27]*Dipartimento di Fisica dell'Università and Sezione INFN, Turin, Italy*
[28]*Dipartimento di Fisica e Astronomia dell'Università and Sezione INFN, Bologna, Italy*
[29]*Dipartimento di Fisica e Astronomia dell'Università and Sezione INFN, Catania, Italy*
[30]*Dipartimento di Fisica e Astronomia dell'Università and Sezione INFN, Padova, Italy*
[31]*Dipartimento di Fisica 'E.R. Caianiello' dell'Università and Gruppo Collegato INFN, Salerno, Italy*
[32]*Dipartimento di Scienze e Innovazione Tecnologica dell'Università del Piemonte Orientale and Gruppo Collegato INFN, Alessandria, Italy*
[33]*Dipartimento Interateneo di Fisica "M. Merlin" and Sezione INFN, Bari, Italy*
[34]*Division of Experimental High Energy Physics, University of Lund, Lund, Sweden*
[35]*Eberhard Karls Universität Tübingen, Tübingen, Germany*
[36]*European Organization for Nuclear Research (CERN), Geneva, Switzerland*
[37]*Excellence Cluster Universe, Technische Universität München, Munich, Germany*
[38]*Faculty of Engineering, Bergen University College, Bergen, Norway*
[39]*Faculty of Mathematics, Physics and Informatics, Comenius University, Bratislava, Slovakia*
[40]*Faculty of Nuclear Sciences and Physical Engineering, Czech Technical University in Prague, Prague, Czech Republic*
[41]*Faculty of Science, P.J. Šafárik University, Košice, Slovakia*
[42]*Faculty of Technology, Buskerud and Vestfold University College, Vestfold, Norway*
[43]*Frankfurt Institute for Advanced Studies, Johann Wolfgang Goethe-Universität Frankfurt, Frankfurt, Germany*
[44]*Gangneung-Wonju National University, Gangneung, South Korea*
[45]*Gauhati University, Department of Physics, Guwahati, India*
[46]*Helsinki Institute of Physics (HIP), Helsinki, Finland*
[47]*Hiroshima University, Hiroshima, Japan*

[48]*Indian Institute of Technology Bombay (IIT), Mumbai, India*
[49]*Indian Institute of Technology Indore, Indore (IITI), India*
[50]*Inha University, Incheon, South Korea*
[51]*Institut de Physique Nucléaire d'Orsay (IPNO), Université Paris-Sud, CNRS-IN2P3, Orsay, France*
[52]*Institut für Informatik, Johann Wolfgang Goethe-Universität Frankfurt, Frankfurt, Germany*
[53]*Institut für Kernphysik, Johann Wolfgang Goethe-Universität Frankfurt, Frankfurt, Germany*
[54]*Institut für Kernphysik, Westfälische Wilhelms-Universität Münster, Münster, Germany*
[55]*Institut Pluridisciplinaire Hubert Curien (IPHC), Université de Strasbourg, CNRS-IN2P3, Strasbourg, France*
[56]*Institute for Nuclear Research, Academy of Sciences, Moscow, Russia*
[57]*Institute for Subatomic Physics of Utrecht University, Utrecht, Netherlands*
[58]*Institute for Theoretical and Experimental Physics, Moscow, Russia*
[59]*Institute of Experimental Physics, Slovak Academy of Sciences, Košice, Slovakia*
[60]*Institute of Physics, Academy of Sciences of the Czech Republic, Prague, Czech Republic*
[61]*Institute of Physics, Bhubaneswar, India*
[62]*Institute of Space Science (ISS), Bucharest, Romania*
[63]*Instituto de Ciencias Nucleares, Universidad Nacional Autónoma de México, Mexico City, Mexico*
[64]*Instituto de Física, Universidad Nacional Autónoma de México, Mexico City, Mexico*
[65]*iThemba LABS, National Research Foundation, Somerset West, South Africa*
[66]*Joint Institute for Nuclear Research (JINR), Dubna, Russia*
[67]*Konkuk University, Seoul, South Korea*
[68]*Korea Institute of Science and Technology Information, Daejeon, South Korea*
[69]*KTO Karatay University, Konya, Turkey*
[70]*Laboratoire de Physique Corpusculaire (LPC), Clermont Université, Université Blaise Pascal, CNRS-IN2P3, Clermont-Ferrand, France*
[71]*Laboratoire de Physique Subatomique et de Cosmologie, Université Grenoble-Alpes, CNRS-IN2P3, Grenoble, France*
[72]*Laboratori Nazionali di Frascati, INFN, Frascati, Italy*
[73]*Laboratori Nazionali di Legnaro, INFN, Legnaro, Italy*
[74]*Lawrence Berkeley National Laboratory, Berkeley, California, USA*
[75]*Moscow Engineering Physics Institute, Moscow, Russia*
[76]*Nagasaki Institute of Applied Science, Nagasaki, Japan*
[77]*National Centre for Nuclear Studies, Warsaw, Poland*
[78]*National Institute for Physics and Nuclear Engineering, Bucharest, Romania*
[79]*National Institute of Science Education and Research, Bhubaneswar, India*
[80]*National Research Centre Kurchatov Institute, Moscow, Russia*
[81]*Niels Bohr Institute, University of Copenhagen, Copenhagen, Denmark*
[82]*Nikhef, Nationaal Instituut voor Subatomaire Fysica, Amsterdam, Netherlands*
[83]*Nuclear Physics Group, STFC Daresbury Laboratory, Daresbury, United Kingdom*
[84]*Nuclear Physics Institute, Academy of Sciences of the Czech Republic, Řež u Prahy, Czech Republic*
[85]*Oak Ridge National Laboratory, Oak Ridge, Tennessee, USA*
[86]*Petersburg Nuclear Physics Institute, Gatchina, Russia*
[87]*Physics Department, Creighton University, Omaha, Nebraska, USA*
[88]*Physics Department, Panjab University, Chandigarh, India*
[89]*Physics Department, University of Athens, Athens, Greece*
[90]*Physics Department, University of Cape Town, Cape Town, South Africa*
[91]*Physics Department, University of Jammu, Jammu, India*
[92]*Physics Department, University of Rajasthan, Jaipur, India*
[93]*Physik Department, Technische Universität München, Munich, Germany*
[94]*Physikalisches Institut, Ruprecht-Karls-Universität Heidelberg, Heidelberg, Germany*
[95]*Purdue University, West Lafayette, Indiana, USA*
[96]*Pusan National University, Pusan, South Korea*
[97]*Research Division and ExtreMe Matter Institute EMMI, GSI Helmholtzzentrum für Schwerionenforschung, Darmstadt, Germany*
[98]*Rudjer Bošković Institute, Zagreb, Croatia*
[99]*Russian Federal Nuclear Center (VNIIEF), Sarov, Russia*
[100]*Saha Institute of Nuclear Physics, Kolkata, India*
[101]*School of Physics and Astronomy, University of Birmingham, Birmingham, United Kingdom*
[102]*Sección Física, Departamento de Ciencias, Pontificia Universidad Católica del Perú, Lima, Peru*
[103]*Sezione INFN, Bari, Italy*
[104]*Sezione INFN, Bologna, Italy*
[105]*Sezione INFN, Cagliari, Italy*
[106]*Sezione INFN, Catania, Italy*

[107] *Sezione INFN, Padova, Italy*
[108] *Sezione INFN, Rome, Italy*
[109] *Sezione INFN, Trieste, Italy*
[110] *Sezione INFN, Turin, Italy*
[111] *SSC IHEP of NRC Kurchatov institute, Protvino, Russia*
[112] *Stefan Meyer Institut für Subatomare Physik (SMI), Vienna, Austria*
[113] *SUBATECH, Ecole des Mines de Nantes, Université de Nantes, CNRS-IN2P3, Nantes, France*
[114] *Suranaree University of Technology, Nakhon Ratchasima, Thailand*
[115] *Technical University of Košice, Košice, Slovakia*
[116] *Technical University of Split FESB, Split, Croatia*
[117] *The Henryk Niewodniczanski Institute of Nuclear Physics, Polish Academy of Sciences, Cracow, Poland*
[118] *The University of Texas at Austin, Physics Department, Austin, Texas, USA*
[119] *Universidad Autónoma de Sinaloa, Culiacán, Mexico*
[120] *Universidade de São Paulo (USP), São Paulo, Brazil*
[121] *Universidade Estadual de Campinas (UNICAMP), Campinas, Brazil*
[122] *University of Houston, Houston, Texas, USA*
[123] *University of Jyväskylä, Jyväskylä, Finland*
[124] *University of Liverpool, Liverpool, United Kingdom*
[125] *University of Tennessee, Knoxville, Tennessee, USA*
[126] *University of the Witwatersrand, Johannesburg, South Africa*
[127] *University of Tokyo, Tokyo, Japan*
[128] *University of Tsukuba, Tsukuba, Japan*
[129] *University of Zagreb, Zagreb, Croatia*
[130] *Université de Lyon, Université Lyon 1, CNRS-IN2P3, IPN-Lyon, Villeurbanne, France*
[131] *V. Fock Institute for Physics, St. Petersburg State University, St. Petersburg, Russia*
[132] *Variable Energy Cyclotron Centre, Kolkata, India*
[133] *Warsaw University of Technology, Warsaw, Poland*
[134] *Wayne State University, Detroit, Michigan, USA*
[135] *Wigner Research Centre for Physics, Hungarian Academy of Sciences, Budapest, Hungary*
[136] *Yale University, New Haven, Connecticut, USA*
[137] *Yonsei University, Seoul, South Korea*
[138] *Zentrum für Technologietransfer und Telekommunikation (ZTT), Fachhochschule Worms, Worms, Germany*

[*] Deceased.
[†] Also at Georgia State University, Atlanta, Georgia, USA.
[‡] Also at Department of Applied Physics, Aligarh Muslim University, Aligarh, India.
[§] Also at M.V. Lomonosov Moscow State University, D.V. Skobeltsyn Institute of Nuclear Physics, Moscow, Russia.